Behavioral/Systems/Cognitive

Olfactory Marker Protein Is Critical for Functional Maturation of Olfactory Sensory Neurons and Development of Mother Preference

Anderson C. Lee, Jiwei He, and Minghong Ma
Department of Neuroscience, University of Pennsylvania School of Medicine, Philadelphia, Pennsylvania 19104

Survival of many altricial animals critically depends on the sense of smell. Curiously, the olfactory system is rather immature at birth and undergoes a maturation process, which is poorly understood. Using patch-clamp technique on mouse olfactory sensory neurons (OSNs) with a defined odorant receptor, we demonstrate that OSNs exhibit functional maturation during the first month of postnatal life by developing faster response kinetics, higher sensitivity, and most intriguingly, higher selectivity. OSNs expressing mouse odorant receptor 23 (MOR23) are relatively broadly tuned in neonates and become selective detectors for the cognate odorant within 2 weeks. Remarkably, these changes are prevented by genetic ablation of olfactory marker protein (OMP), which is exclusively expressed in mature OSNs. Biochemical and pharmacological evidence suggests that alteration in odorant-induced phosphorylation of signaling proteins underlie some of the $OMP^{-/-}$ phenotypes. Furthermore, in a novel behavioral assay in which the mouse pups are given a choice between the biological mother and another unfamiliar lactating female, wild-type pups prefer the biological mother, while OMP knock-out pups fail to show preference. These results reveal that OSNs undergo an OMP-dependent functional maturation process that coincides with early development of the smell function, which is essential for pups to form preference for their mother.

Introduction

Many altricial animals give birth to close-eyed and relatively immobile pups, with early survival relying critically on the sense of smell. When olfactory function is genetically disrupted in mice, the pups die shortly after birth from inability to suckle (Brunet et al., 1996; Belluscio et al., 1998; Wong et al., 2000). Curiously, the olfactory system is relatively immature at birth and undergoes significant development postnatally. Newborn rodents continue to improve odor detection abilities (Alberts and May, 1980b) and develop preference for familiar odors signaling mother, siblings, home, and food (Schapiro and Salas, 1970; Gregory and Pfaff, 1971; Galef and Henderson, 1972; Alberts and Brunjes, 1978; Brunjes and Alberts, 1979; Polan and Hofer, 1998). Associative learning based on olfactory cues in early life effectively modifies the brain circuits leading to behavioral attraction or avoidance (Moriceau and Sullivan, 2006).

Odor detection relies on a large family of odorant receptors (ORs) expressed in olfactory sensory neurons (OSNs) within the neuroepithelium of the nose. Binding of odor molecules to ORs leads to increased intracellular cAMP levels via sequential activation of olfactory G-protein (G_{olf}) and type III adenylyl cyclase (ACIII). Subsequent opening of a cyclic nucleotide-gated (CNG) channel and a Ca^{2+}-activated Cl^- channel depolarizes OSNs which then fire action potentials transmitting odor information to the olfactory bulb in the brain (Su et al., 2009; Touhara and Vosshall, 2009). OSNs from embryos or neonates are capable of responding to odorants (Gesteland et al., 1982; Belluscio et al., 1998). However, little is known about how these neurons mature functionally during the postnatal life.

Olfactory marker protein (OMP) is widely recognized as a molecular marker for mature OSNs (Margolis, 1972). Genetic deletion of OMP results in slower odorant response kinetics revealed by electroolfactogram (EOG), single-cell recording, and calcium imaging (Buiakova et al., 1996; Ivic et al., 2000; Reisert et al., 2007; Kwon et al., 2009). Behaviorally, $OMP^{-/-}$ mice exhibit reduced odorant sensitivity and altered odor discrimination (Youngentob and Margolis, 1999; Youngentob et al., 2001, 2004). Because OMP expression is developmentally regulated, starting at embryonic day 14 and reaching the adult level at postnatal day 30 (P30) (Graziadei et al., 1980), it is tempting to hypothesize that OMP plays a role in functional maturation of OSNs.

Here we investigated whether OSNs expressing a defined OR [mouse odorant receptor 23 (MOR23)] with a known ligand (lyral) exhibit functional changes during the first postnatal month. Using patch-clamp recordings, we demonstrated that MOR23 neurons from P30 mice show faster response kinetics, higher sensitivity, and higher selectivity than those from P0 mice. Remarkably, OMP is required for this maturation process. Bio-

Received Sept. 27, 2010; revised Dec. 13, 2010; accepted Dec. 27, 2010.

This work was supported by the National Institute on Deafness and Other Communication Disorders, National Institutes of Health (R01 DC006213 to M.M. and fellowship to A.C.L.). We are grateful to Drs. Stephen Moss and Miho Terunuma for guidance and equipment in obtaining the biochemical data. We thank Dr. Rui Feng and Yun Rose Li for their advice and help with the statistical analysis, Kim Kridsada for her technical assistance in the behavioral tests, and Drs. Huikai Tian and Tim Connelly for insightful discussions.

Correspondence should be addressed to Dr. Minghong Ma, Department of Neuroscience, University of Pennsylvania School of Medicine, 215 Stemmler Hall, 3450 Hamilton Walk, Philadelphia, PA 19104. E-mail: minghong@mail.med.upenn.edu.

A. C. Lee's present address: Department of Biochemistry and Molecular Biophysics and Howard Hughes Medical Institute, Columbia University, New York, NY 10032. E-mail: al2919@columbia.edu.

DOI:10.1523/JNEUROSCI.5067-10.2011

 0270-6474/11/312974-09$15.00/0

chemical and pharmacological evidence supports our hypothesis that altered ACIII phosphorylation contributes to the $OMP^{-/-}$ phenotype. Furthermore, when pups are given a choice between the biological mother and another unfamiliar lactating female, wild-type but not $OMP^{-/-}$ pups prefer the former to suckle or huddle. These results reveal that OSNs undergo an OMP-dependent functional maturation process that coincides with the postnatal development of the smell function necessary for the survival of altricial mice.

Materials and Methods

Animals. Genetically targeted MOR23-IRES (internal ribosome entry site)-tauGFP mice were used to record MOR23 neurons that coexpress green fluorescent protein (GFP) (Vassalli et al., 2002). To obtain $OMP^{-/-}$ MOR23 neurons, MOR23-IRES-tauGFP and OMP-synapto-pHluorin (spH) mice (the coding region of *OMP* was replaced by that of spH) (Bozza et al., 2004) were bred to generate homozygous double mutant mice. All mice were in a mixed 129 and C57BL/6 genetic background and tested at ages from P0 to P30 as specified. P0 mice were obtained by checking breeding pairs for new litters at 12 h intervals, and the experiments were done within 12 h of detection to ensure recorded cells were from pups within 24 h of birth. All procedures were approved by the Institutional Animal Care and Use Committee at the University of Pennsylvania.

Patch clamp. Intact epithelial preparations were as in our published procedures (Ma et al., 1999; Grosmaitre et al., 2006). Mice were deeply anesthetized either by intraperitoneal injection of ketamine/xylazine (200 mg/kg and 15 mg/kg respectively) or 10 min incubation on ice (P0 and P7 pups), and then decapitated. The head was immediately put into ice-cold Ringer's solution, which contained (in mM): 124 NaCl, 3 KCl, 1.3 $MgSO_4$, 2 $CaCl_2$, 26 $NaHCO_3$, 1.25 NaH_2PO_4, 15 glucose, pH 7.6, and 305 mOsm. The pH was kept at 7.4 after bubbling with 95% O_2 and 5% CO_2. The nose was dissected out en bloc, the olfactory mucosa attached to the nasal septum and the dorsal recess was removed and kept in oxygenated Ringer. Before use, the entire mucosa was peeled away from the underlying bone and transferred to a recording chamber with the mucus layer facing up. While recording, oxygenated Ringer was continuously perfused at 25 ± 2°C.

The dendritic knobs of OSNs were visualized through an upright microscope (Olympus BX61WI) with a 40× water-immersion objective. An extra 4× magnification was achieved by an accessory lens in the light path. The GFP-tagged cells were visualized under fluorescent illumination. Superimposition of the fluorescent and bright-field images allowed identification of the fluorescent cells under bright field, which directed the recording pipettes. Electrophysiological recordings were controlled by an EPC-9 amplifier combined with Pulse software (HEKA). Perforated patch clamp was performed on the dendritic knobs by including 260 μM nystatin in the recording pipette, which was filled with the following solution (in mM): 70 KCl, 53 KOH, 30 methanesulfonic acid, 5.0 EGTA, 10 HEPES, 70 sucrose, pH 7.2 (KOH), and 310 mOsm. Under voltage-clamp mode, the signals were initially filtered at 10 kHz and then at 2.9 kHz. For odorant-induced transduction currents (which are slow and long lasting), the signals were sampled at 333 Hz. Further filtering offline at 60 Hz (to remove noise) did not change the response kinetics or amplitudes, indicating that the sampling rate was sufficient and signal aliasing was not a concern.

A seven-barrel pipette was used to deliver stimuli by pressure ejection through a picospritzer (Pressure System IIe). The stimulus pipette was placed ~20 μm downstream from the recording site, and both mechanical and chemical responses could be elicited in some neurons (Grosmaitre et al., 2007). All stimuli were delivered by 20 psi (138 kPa) via a picospritzer. The pulse length was kept at 300 ms to ensure that the neurons were stimulated by the intrapipette concentration (Grosmaitre et al., 2006).

Odorants were prepared fresh daily in Ringer's. Lyral was provided as a generous gift from International Fragrances and Flavors, while (−)-carvone, eugenol, heptanal, and geraniol were purchased from Sigma-Aldrich. Myristoylated autocamtide-2-related inhibitory peptide (AIP) was purchased from Calbiochem and prepared before each experiment from 1000× DMSO stock. Okadaic acid (OA) was from Calbiochem and prepared before each experiment from 100× Ringer stock.

Behavioral tests. Three- to 6-month-old MOR23-IRES-tauGFP [wild type (WT)] or OMP-spH/MOR23-IRES-tauGFP ($OMP^{-/-}$) male and female mice were paired to produce litters. Behavioral assays were conducted between 10:00 A.M. and 12:00 P.M. in an isolated room on a 7:00 A.M.–7:00 P.M. light cycle. For each assay, a clean mouse cage (8 × 12 inches) was used with cardboard barriers surrounding the cage and even illumination to minimize environmental distractions. Two testing mothers (called the stimulus animals) were anesthetized with ketamine/xylazine (200 and 15 mg/kg, respectively) and placed 5–10 cm apart symmetrically across the midline of the cage. For each assay, untrained test pups between the age of P7 and P16 were placed in between stimulus animals and allowed to explore freely. Pups were tested individually or in groups (up to 6 at a time), and both approaches produced similar results. Sometimes the same pups were retested and similar results were always obtained as in the initial test. Videotaping (Logitech QuickCam Pro 9000) was performed for 5–10 min until pups settled for >3 min (most pups chose a position to suckle or huddle within 2–5 min) and preference was judged at the final position. The experiments were terminated and the data were excluded if the animals did not stop exploring after 10 min or fell asleep without exploring.

Isolation of ciliary membranes from OSNs. Ciliary membranes were isolated using the high calcium method with minor modifications (Pace et al., 1985; Sklar et al., 1986). The nasal epithelia from P30 mice were surgically excised and pooled in 9 ml of solution C (in mM: 120 NaCl, 5 KCl, 1.6 K_2HPO_4, 1.2 $MgSO_4$, 25 $NaHCO_3$, 7.5 D-glucose, adjusted to pH 7.4). All steps were performed at 4°C if not otherwise stated. The pooled tissue was allowed to settle to the bottom of the tube and the supernatant was discarded. The tissue was resuspended in 5 ml of solution C containing 10 mM $CaCl_2$ (solution D). Solution D was prepared by slowly adding $CaCl_2$ to a final concentration of 10 mM while gassing with 5% CO_2/95% air at 22°C to prevent Ca_2PO_4 from precipitation. The tissue was rocked for 20 min (as in the mechanical agitation method) and then centrifuged at 7700 × *g* for 5 min. This supernatant was reserved in a new tube for subsequent pooling with membranes dislodged in a second rocking step. The pellet was resuspended in 4 ml of solution D and rocked for a second time for 20 min. Supernatant from this step, collected by centrifugation at 7700 × *g* for 5 min, was added to the supernatant from the first calcium shock incubation. The combined supernatant was centrifuged for 15 min at higher speed (27 000 × *g*), supernatant was discarded, and resuspended in TEM buffer (10 mM Tris-HCl, 3 mM $MgCl_2$, 2 mM EDTA, pH 8.0) and stored at −70°C. Protein was determined by the Bradford Assay (Bio-Rad), with bovine serum albumin as standard.

Immunoblot analysis. Membrane proteins were separated on 8% SDS-polyacrylamide gels and transferred to Hybond-C nitrocellulose membranes (GE Healthcare). Nonspecific binding sites were blocked with 5% dry nonfat milk (Carnation) in TBST (10 mM Tris-HCl, pH 8.0, 150 mM NaCl, and 0.4% Tween 20) for 1 h at room temperature. The blots were incubated with primary antibody for 1 h at room temperature or overnight at 4°C. The primary antibodies used were rabbit anti-ACIII (1:1000; Santa Cruz Biotechnology, sc-588), rabbit anti-G_{olf} (1:1000; Santa Cruz Biotechnology, sc-385), rabbit anti-phosphodiesterase 1C (PDE1C) (1:1000; Abcam, ab14602), rabbit anti-PDE4A (1:1000; Abcam, ab14607), mouse anti-β-arrestin-2 (1:1000; Santa Cruz Biotechnology, sc-13140), and mouse anti-β-actin (1:5000; Sigma, A5441). Blots were washed three times with TBST and then incubated with horseradish peroxidase (HRP)-conjugated secondary antibody for 1 h at room temperature. The secondary antibodies used were HRP-conjugated anti-rabbit antibody (1:5000; Millipore) and HRP-conjugated anti-mouse antibody (1:5000; Millipore). Blots were washed twice with TBST and once with TBS (10 mM Tris-HCl, pH 8.0, 150 mM NaCl). ECL (Pierce) was used to visualize bound antibodies. Blots were then quantified using the CCD-based FujiFilm LAS 3000 system.

Phosphorylation of ACIII. Purified cilia (4 μg) were resuspended with 50 μl of phosphorylation buffer containing (in mM): 50 HEPES-NaOH, 10 magnesium acetate, 0.5 $CaCl_2$, pH 7.5. After incubation at 30°C for 1 min, cilia were treated with 10 μCi [γ-^{32}P]ATP (specific activity, 3000 Ci/mmol; PerkinElmer) for another 1 min and then treated with a mix-

ture of 19 odorants each at 10 μM [heptanol, octanol, hexanal, heptanal, octanal, heptanoic acid, octanoic acid, cineole, amyl acetate, (+)-limonene, (−)-limonene, (+)-carvone, (−)-carvone, 2-heptanone, anisaldehyde, benzaldehyde, acetophenone, 3-heptanone, and ethyl vanilline) for 1 min. To terminate the reaction, 450 μl of cell lysis buffer (containing, in mM: 20 Tris-HCl, pH 8.0, 150 NaCl, 5 EDTA, 1% Triton X-100, 1 μg/ml leupeptin, 1 μg/ml aprotinin, and 0.5 phenylmethylsulfonyl fluoride) were added and rotated for 1 h at 4°C. Lysates were then mixed with 2 μg of anti-ACIII antibody (Santa Cruz Biotechnology) and protein A-Sepharose (20 μl of 50% slurry; GE Healthcare) and gently rotated for overnight at 4°C. The beads were precipitated by centrifugation and washed twice with 1 ml of cell lysis buffer, three times with 1 ml of washing buffer containing (in mM): 20 Tris-HCl, pH 8.0, 500 NaCl, 5 EDTA, 1% Triton X-100, and three times with 1 ml of cell lysis buffer. After the final wash, the beads were resuspended in 50 μl of a sample buffer for SDS-PAGE, followed by an electrophoresis, autoradiography, and analysis with a phosphor imager (Bio-Rad).

Statistical analysis. Three-way ANOVA tests, Bonferroni multiple-comparisons tests, logistic regression analysis, and χ^2 tests were performed using R Program. Dose–response curves were fit by GraphPad Prism software. Student's *t* tests were performed using a built-in function in Excel (Microsoft). An average is shown as mean ± SE unless otherwise stated.

Results

OSNs exhibit faster response kinetics during development

To test whether OSNs undergo functional changes during development, we measured odorant responses in individual neurons from animals at different ages (P0–P30). We used a previously characterized, gene-targeted mouse line (MOR23-IRES-tauGFP) in which MOR23-expressing OSNs coexpress GFP (Vassalli et al., 2002). For simplicity of description, these "green" cells are called WT-MOR23 neurons in contrast to *OMP*$^{-/-}$ MOR23 neurons. Perforated patch-clamp recordings were performed on the dendritic knobs of individual OSNs in the intact epithelia (Grosmaitre et al., 2006).

First, we evaluated developmental changes in response kinetics and recorded a total of 73 WT-MOR23 neurons from P0, P7, and P30 mice (n = 30, 21, and 22 cells, respectively). We quantified the following parameters: latency, rise time, peak current, decay time, and residual current measured 10 s after the stimulation (Fig. 1*A*). During the first postnatal month, the response kinetics of WT-MOR23 neurons became significantly faster (Figs. 1*B*, 2). When stimulated by 10 μM lyral, the rise time changed from 0.58 ± 0.11 s (P0, n = 30) to 0.22 ± 0.04 s (P30, n = 22) or shortened by 62% (Fig. 1*C*), and the residual current ratio ($I_{residual}/I_{peak}$) changed from 0.21 ± 0.05 (P0) to 0.08 ± 0.03 (P30), a 62% reduction (Fig. 1*D*). Note that the response kinetics depended on the odorant concentration within each age group and similar trends were generally observed for the decay time and the residual current ratio (Fig. 2). These results indicate that WT-MOR23 neurons from P30 animals have both faster activation and faster decay in odorant-elicited responses when compared with their counterparts from neonates.

OMP deletion results in OSNs with slow response kinetics

To study the effects of OMP deletion on functional properties of OSNs, we generated homozygous *OMP*$^{-/-}$ mice with GFP labeled MOR23 neurons. Gene-targeted MOR23-IRES-tauGFP and OMP-spH mice (Bozza et al., 2004) were bred to generate homozygous double mutant mice. Note that the fluorescent spH molecule is primarily expressed in the axon terminals of OSNs, which allows unambiguous identification of GFP signals in the cilia and dendritic knobs of MOR23 neurons in the olfactory epithelium. We refer to these "green" cells as *OMP*$^{-/-}$ MOR23

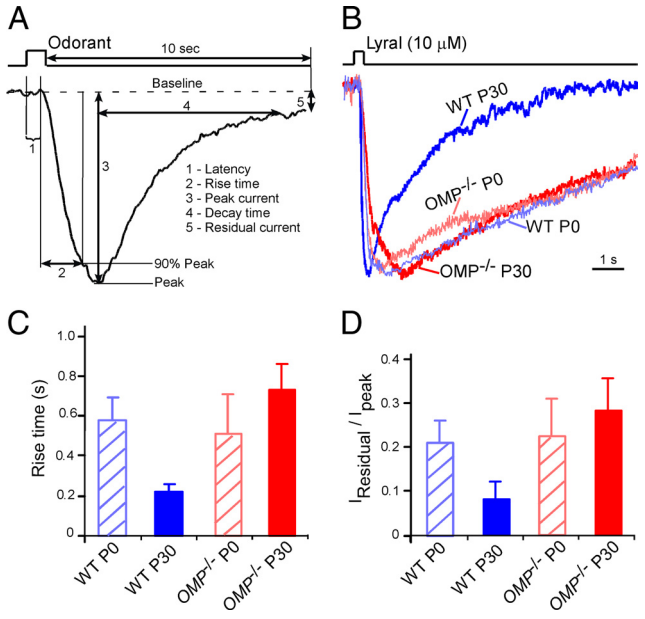

Figure 1. Wild-type but not *OMP*$^{-/-}$ MOR23 neurons develop faster response kinetics during the first month. ***A***, Analysis of odorant-induced transduction currents under voltage-clamp mode. The latency (1) is the time between the onset of the stimulus and the starting point of the response. The rise time (2) is the time it takes for the current to reach 90% of the peak (3) from the starting point of the response. The decay time (4) is the time it takes for the current to return to 10% of the peak from the peak. Since some responses take minutes to return to the baseline, a "residual" current (5) is measured 10 s after the stimulation. ***B***, Inward currents (normalized to the same peak) were elicited by lyral pulses from MOR23 neurons under different conditions: WT P0 (thin blue), WT P30 (thick blue), *OMP*$^{-/-}$ P0 (thin red) and *OMP*$^{-/-}$ P30 (thick red). Representative traces from four single neurons were aligned at the start of the responses. ***C***, ***D***, The rise time (***C***) and the ratio of the residual current to the peak (***D***) are summarized for the four conditions: WT P0, WT P30, *OMP*$^{-/-}$ P0, and *OMP*$^{-/-}$ P30. The holding potential was −65 mV for all neurons. The output of the statistical analysis using three-way ANOVA is detailed in Figure 2*D*.

neurons. We recorded a total of 38 *OMP*$^{-/-}$ MOR23 neurons: 11 from P0, 10 from P7, and 17 from P30 mice. Unlike WT-MOR23 neurons, *OMP*$^{-/-}$ MOR23 neurons did not show significant changes in response kinetics from P0 to P30 (Fig. 1*B*). When stimulated by 10 μM lyral, the rise time was 0.47 ± 0.20 s (n = 11) at P0 and 0.73 ± 0.13 s (n = 17) at P30 (Fig. 1*C*), and the residual current ratio ($I_{residual}/I_{peak}$) was 0.22 ± 0.08 at P0 and 0.28 ± 0.07 at P30 (Fig. 1*D*). The lack of change in the response kinetics was also observed with 1 and 100 μM lyral applications (Fig. 2*A–C*). Three-way ANOVA tests revealed that the activation phase (rise time) depended on age and OMP status, while the decay phase (decay time and $I_{residual}/I_{peak}$) depended on age, OMP status and concentration (Fig. 2*D*). The statistical analysis also confirmed that lyral at higher concentrations induced responses with shorter latency and higher peak current in all groups as expected (Fig. 2*D*). Generally, *OMP*$^{-/-}$ MOR23 neurons at P30 responded to lyral similarly to WT-MOR23 neurons at P0, but with significantly slower kinetics than their WT counterparts at P30, suggesting that OMP is necessary for the kinetic changes during development.

The signaling deficits of OMP deletion may be wide ranging, but a recent study suggests that the action sites are upstream of the CNG channel activation (Reisert et al., 2007). We examined the protein levels of five key components (G_{olf}, ACIII, PDE1C, PDE4A and β-arrestin-2) in the signal transduction cascade and found a significant upregulation of the ACIII level (Fig. 3*A*,*B*). Odor-induced phosphorylation, and subsequent inactivation of

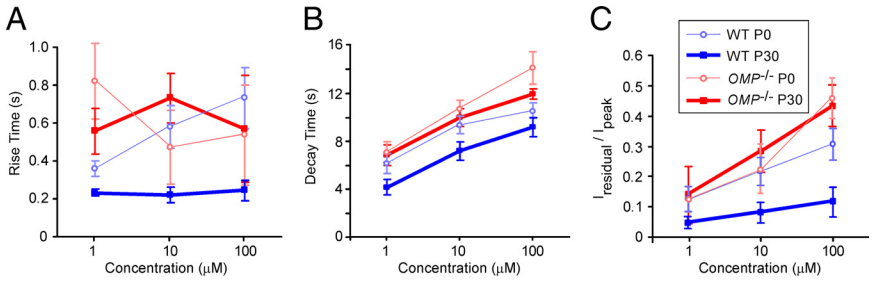

D

Three-way ANOVA output

	Age		OMP status		Concentration	
Parameter	F	p	F	p	F	p
Rise Time	8.66	**0.0035**	8.44	**0.0040**	0.84	0.3590
Decay Time	14.96	**< 0.001**	40.49	**< 0.001**	117.95	**< 0.001**
$I_{residual}/I_{peak}$	9.86	**0.0019**	37.48	**< 0.001**	37.36	**< 0.001**
Latency	2.65	0.1040	12.43	**< 0.001**	17.66	**< 0.001**
Peak Current	9.57	**0.0022**	0.76	0.383	23.90	**< 0.001**

Figure 2. The response kinetics of MOR23 neurons depends on age, OMP status, and concentration. ***A–C***, Summary of the rise time (***A***), the decay time (***B***), and the ratio of the residual current to the peak (***C***) under different conditions: WT P0, WT P30, *OMP*$^{-/-}$ P0, and *OMP*$^{-/-}$ P30. All neurons were recorded under voltage-clamp mode with a holding potential of −65 mV. Not shown are P7 data, which generally fall in between P0 and P30 data. ***D***, Comparison of all five parameters is performed by three-way ANOVA tests based on age (coded as an ordinal variable with levels 1, 2, and 3 corresponding to P0, P7, and P30, respectively), OMP status (coded as a categorical variable), and concentration (coded as an ordinal variable with level 1, 2 and 3 corresponding to 1, 10 and 100 μM, respectively). Significant *p* values are in bold. A significant *p* value in OMP status indicates difference between WT and *OMP*$^{-/-}$ mice. A significant *p* value in age (or concentration) indicates that an increment in age (or concentration) increases or decreases the parameter. Other significant differences not detailed in the main text include a longer latency of the responses in *OMP*$^{-/-}$ neurons than in WT neurons and a decrease in peak currents with age.

ACIII by Ca^{2+}/calmodulin kinase II (CaMKII) contributes to response termination (Wei et al., 1998). We reasoned that the long-lasting responses observed in *OMP*$^{-/-}$ neurons could result from less ACIII phosphorylation, which leads to slower termination (Fig. 3*C*). We indeed observed a reduction in phosphorylation of ACIII using a biochemical assay (Fig. 3*D*). We expected that blocking CaMKII (thus reducing ACIII phosphorylation) would prolong the response decay in WT-MOR23 neurons, mimicking the *OMP*$^{-/-}$ phenotype. When a membrane-permeable CaMKII inhibitor, AIP (1 μM), was included in Ringer's solution, WT-MOR23 neurons at P30 exhibited slow decay ($I_{residual}/I_{peak} = 0.21 \pm 0.07$, $n = 4$) (Fig. 3*E*,*G*, magenta). After 1 h washout of AIP, WT-MOR23 neurons showed faster decay ($I_{residual}/I_{peak} = 0.02 \pm 0.01$, $n = 4$) (Fig. 3*E*,*G*, green) with parameters similar to the untreated controls (Fig. 1*B*, thick blue). Conversely, we expected that blocking phosphatase activity (Boekhoff and Breer, 1992; Kroner et al., 1996), thus increasing ACIII phosphorylation, would shorten the response decay of *OMP*$^{-/-}$ MOR23 neurons, reversing the *OMP*$^{-/-}$ phenotype. When a phosphatase inhibitor, OA (at 1 μM), was included in Ringer's solution, *OMP*$^{-/-}$ MOR23 neurons at P30 exhibited faster decay ($I_{residual}/I_{peak} = 0.02 \pm 0.02$, $n = 5$) (Fig. 3*F*,*G*, green), similar to WT-MOR23 neurons at P30 (Fig. 1*B*, thick blue). After 1 h washout of OA, *OMP*$^{-/-}$ MOR23 neurons showed slow decay ($I_{residual}/I_{peak} = 0.28 \pm 0.06$, $n = 4$) (Fig. 3*F*,*G*, green), similar to untreated *OMP*$^{-/-}$ MOR23 neurons at P30 (Fig. 1*B*, thick red). The results reveal that reducing phosphorylation by blocking CaMKII is sufficient to slow the response decay, while increasing phosphorylation by blocking phosphatase activity is sufficient to hasten the response decay. Although we cannot rule out the possibility that AIP and OA exert their actions on targets other than ACIII, these results support our hypothesis. Modification of ACIII (and/or other proteins) phosphorylation states may be one mechanism underlying the *OMP*$^{-/-}$ phenotype.

WT but not *OMP*$^{-/-}$ OSNs exhibit higher sensitivity during development

Next, we examined whether the sensitivity of WT-MOR23 neurons changes during the first postnatal month. WT-MOR23 neurons from P0 and P30 mice were stimulated by lyral at different concentrations (0.01, 1, 10 and 100 μM) with an interval > 1 min to minimize odorant adaptation (Fig. 4*A*,*B*). For each cell, the peak current induced under each concentration is normalized to the maximum peak current (typically induced by 100 μM lyral). A single dose–response curve is then fit based on the data from all neurons within each age group, using a modified Hill equation, $I_{norm} = (I - I_{baseline})/I_{max} = 1/(1 + (K_{1/2}/C)^n$, where I represents the peak current, $I_{baseline}$ the nonzero mechanical response induced by a Ringer puff (Grosmaitre et al., 2007), I_{max} the maximum current induced by the saturating concentration, $K_{1/2}$ the concentration at which half of the maximum response was reached, C the concentration of lyral, and n the Hill coefficient. The mean $K_{1/2}$ value shifted from 3.5 μM ($n = 11$) at P0 to 0.6 μM ($n = 8$) at P30 (Fig. 4*E*,*F*), indicating that WT-MOR23 neurons become more sensitive during the first month. We then obtained the dose–response curves for *OMP*$^{-/-}$ MOR23 neurons (Fig. 4*C*,*D*). The $K_{1/2}$ value was 5.8 μM at P0 ($n = 4$) and 4.2 μM at P30 ($n = 10$), not significantly different from each other, but significantly higher than the WT P30 value (Fig. 4*E*,*F*). Thus *OMP*$^{-/-}$ MOR23 neurons fail to increase their sensitivity by P30.

WT but not *OMP*$^{-/-}$ MOR23 neurons at P30 become selective lyral detectors

Last, we tested whether the selectivity of OSNs changes during the first postnatal month. In addition to lyral, we stimulated MOR23 neurons with four other odorants with distinct structural features: (−)-carvone, eugenol, geraniol and heptanal at 100 μM if not otherwise stated (Fig. 5). Only cells that were tested by the complete set of five odorants plus Ringer are included in the following analysis. Confirming earlier identification of lyral as the cognate ligand of MOR23 (Touhara et al., 1999), all WT-MOR23 neurons at P30 ($n = 9$) responded to lyral (Fig. 5*C*), and only two cells displayed responses to a nonlyral odorant with peak amplitude > 10% of the lyral response. Remarkably, WT-MOR23 cells ($n = 9$) from P0 mice responded to many odorants and were not specifically tuned to lyral (Fig. 5*A*). Nine of nine cells (100%) responded to a nonspecific ligand with peak amplitude > 10% of the lyral response, with five of these cells responding to a nonspecific ligand greater than the lyral response. We then tested WT-MOR23 cells from P9–P15 mice (age matched to the behavioral tests described below), which were similar to their counterparts from P30 mice (Fig. 5*B*). These data reveal that WT-MOR23 neurons, which are relatively nonselective at birth, undergo a maturation process in their ligand selectivity and become selective lyral detectors postnatally. We then tested whether OMP is necessary for the selectivity change observed in WT-

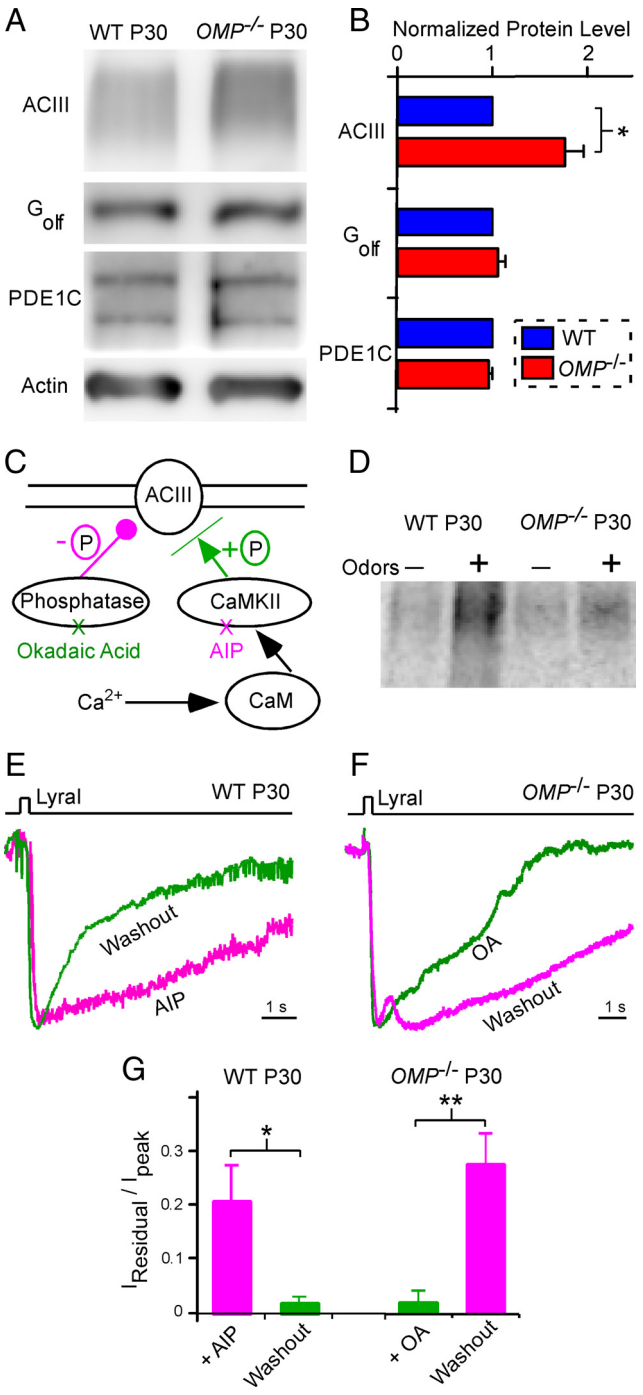

Figure 3. Deletion of OMP alters ACIII signaling. ***A***, The signaling proteins from the olfactory epithelia obtained from WT and $OMP^{-/-}$ P30 mice were stained by specific antibodies in Western blots. Three of the five tested proteins are shown here. Note that ACIII protein has a smear-like band according to the manufacture's datasheet. ***B***, The expression levels of three signaling proteins in $OMP^{-/-}$ mice are normalized to those in WT animals. The ACIII level in the olfactory epithelium was ~75% higher in $OMP^{-/-}$ mice ($n = 5$ samples) with adjusted $p < 0.05$ (*) in *t* test with Bonferroni correction. ***C***, Schematic drawing illustrates that phosphorylation of ACIII by CaMKII inhibits its enzyme activity, while dephosphorylation by phosphatase resets its activity. Phosphorylation and dephosphorylation are represented by green and magenta, respectively. ***D***, OMP deletion reduced odorant-induced ACIII phosphorylation. ACIII phosphorylation was measured by incubating purified olfactory cilia with (+) or without (−) an odorant mixture with [γ-^{32}P]ATP for 1 min. ACIII protein was immunoprecipitated and resolved with SDS-PAGE, and radiolabeled phospho-ACIII was visualized on x-ray film. Basal ACIII phosphorylation was ~10% higher in $OMP^{-/-}$ mice. Odorant-induced phosphorylation of ACIII increased by ~2.3-fold in WT animals, and only ~1.5 in $OMP^{-/-}$ animals. Similar results were obtained from two samples. Considering that ACIII protein is upregulated in $OMP^{-/-}$ mice (***A***, ***B***), the reduction in phosphorylated ACIII in $OMP^{-/-}$ mice is even more significant. ***E***, Block of ACIII phosphorylation via inhibition of CaMKII slows odorant response decay in WT-MOR23 neurons from P30 mice. Inward currents (normalized to the same peak) were elicited by brief lyral (10 μM) pulses in the presence of 1 μM AIP (magenta) and after washout (green). ***F***, Block of ACIII dephosphorylation via inhibiting phosphatase activity hastens odor response decay in $OMP^{-/-}$ MOR23 neurons from P30 mice. Inward currents (normalized to the same peak) were elicited by brief lyral (10 μM) pulses in the presence of 1 μM OA (green) and after washout (magenta). The holding potential was −65 mV for all neurons. ***G***, The ratio of the residual current to the peak is summarized for the four conditions in ***E*** and ***F***. Unpaired Student's *t* test (assuming equal variances and two-tail) is used: *$p < 0.05$ and **$p < 0.01$.

MOR23 neurons during development. Similar to their WT counterparts, all nine $OMP^{-/-}$ MOR23 neurons from P0 mice responded to multiple odorants (Fig. 5*D*) and 89% (8 of 9) of the cells responded to a nonspecific ligand with peak amplitude > 10% of the lyral response. Strikingly, most $OMP^{-/-}$ MOR23 neurons from P9–P15 or from P30 mice continued to respond to many nonspecific odorants instead of being specifically tuned to lyral (Fig. 5*E*,*F*). Sixty-seven percent (12 of 18) and 88% (14 of 16) of the cells from P9–P15 and P30 $OMP^{-/-}$ mice, respectively, responded to another ligand with peak amplitude > 10% of lyral response. All three $OMP^{-/-}$ groups contained some cells responding to a nonspecific ligand greater than the lyral response (Fig. 5*D*–*F*). Using logistic regression analysis, we compared the percentage of cells responding to a nonlyral odorant with peak amplitude > 10% of the lyral response in different groups. The analysis showed that age and OMP status are two critical factors in determining the tuning property of MOR23 neurons. P0 groups are more likely to be broadly responsive compared with P30 groups (odds ratio = 21.4, $p < 0.05$), whereas P9–P15 groups are similar to P30 groups. $OMP^{-/-}$ groups are more likely to be broadly responsive than the WT groups (odds ratio = 12.4, $p < 0.001$). These data indicate that $OMP^{-/-}$ MOR23 neurons fail to become specific lyral detectors by P30.

WT but not $OMP^{-/-}$ pups prefer the biological mother

Since OSNs undergo functional maturation during the first month of life, we expected to observe some behavioral deficits in the development of smell function. We devised a maternal preference assay to test the ability of pups to discriminate their biological mother from another lactating but unfamiliar female. The two mothers were anesthetized and placed 5–10 cm apart in the center of a clean cage (Fig. 6*A*,*B*). The test pups aged P7–P16 were placed between the stimulus animals and allowed to explore the cage freely. Pups younger than P7 were generally not active enough, while those older than P16 often did not stop exploring the new environment within 10 min. With both mothers anesthetized, vocalization, retrieval and temperature influences are eliminated, and the behavior of pups is driven primarily by olfactory cues. Most pups attempted to suckle within 2–5 min, and preference was determined by the position of the pup nose relative to the midline after they settled (Fig. 6*A*,*B*). To ensure that the WT and $OMP^{-/-}$ pups were tested under similar conditions, one WT and one $OMP^{-/-}$ mother were paired in most of the experiments and their age matched pups were tested consecutively. Most of the WT pups (78%, $n = 45$ pups from 7 litters) preferred to suckle or huddle with their biological mother over the unfamiliar lactating female (Fig. 6*A*,*C*). Remarkably, $OMP^{-/-}$ pups failed to show maternal preference, with 55% ($n = 58$ from 9 litters) suckling or huddling with their biological mother (Fig. 6*B*,*C*). To rule out that this finding was due to some deficits of the $OMP^{-/-}$ mothers, we also performed the same test

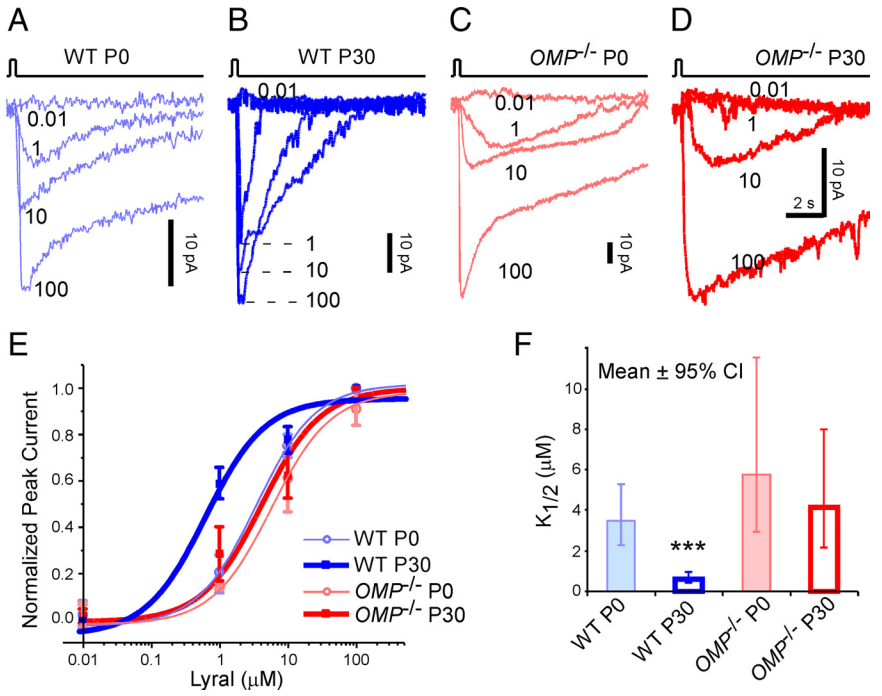

Figure 4. Wild-type but not $OMP^{-/-}$ MOR23 neurons increase the sensitivity to lyral during the first month. ***A–D***, Inward currents were induced by lyral at various concentrations (0.01–100 μM) under different conditions: WT P0 (***A***), WT P30 (***B***), $OMP^{-/-}$ P0 (***C***), and $OMP^{-/-}$ P30 (***D***). The holding potential was −65 mV for all neurons. The traces were from four individual neurons. ***E***, The dose–response curves are plotted for different conditions. ***F***, The $K_{1/2}$ value is summarized for different conditions. We performed Bonferroni multiple comparisons for log$K_{1/2}$ among the four groups. MOR23 has significantly lower log$K_{1/2}$ compared with the other three groups (***adjusted $p < 0.001$ for all 3 comparisons), whereas there is no difference among the other three. For easier comprehension, the mean $K_{1/2} \pm 95\%$ confidence interval (CI) is plotted here.

using two WT mothers. Similar preference was obtained in the WT pups (81% or 21 of 26 from four litters). Additional control experiments revealed that mouse pups (WT or $OMP^{-/-}$) preferred lactating females over nonlactating females (both are unfamiliar; Fig. 6*C*), confirming that $OMP^{-/-}$ pups did not have deficits in finding lactating nipples or suckling. These results suggest that OMP-dependent maturation of OSNs is necessary for mouse pups to develop preference for the biological mother.

Discussion

Here we report that mouse OSNs undergo a functional maturation process by showing faster response kinetics, higher sensitivity, and higher selectivity from P0 to P30. Genetic ablation of OMP prevents the response property changes during postnatal development, indicating a critical role of OMP in functional maturation of OSNs. Altered odorant-induced phosphorylation of ACIII may provide a molecular and cellular mechanism underlying the slow decay observed in $OMP^{-/-}$ neurons. In a mother preference assay, WT pups prefer their biological mother over another unfamiliar lactating female, while $OMP^{-/-}$ pups fail to show preference. The current study reveals OMP-dependent functional maturation of OSNs that coincides with the postnatal development of the smell function.

To examine functional alterations of OSNs during postnatal development, we compared the odorant responses of MOR23 neurons from mice at different ages (P0 to P30). Our data indeed reveal significant changes in the following three aspects, which potentially improve the smell function. OSNs exhibit faster activation and decay kinetics in responding to odorants during postnatal development (Figs. 1, 2). Interestingly, such changes coincide with the postnatal increment of the sniffing rate in rodents (Welker, 1964; Alberts and May, 1980a) and may allow OSNs to faithfully detect odorants at a higher frequency. In addition, OSNs exhibit higher sensitivity during postnatal development (Fig. 4). The dynamic range of MOR23 neurons in responding to lyral covers 3–4 orders of magnitude in all age groups, but the averaged $K_{1/2}$ value changes from 3.5 μM at P0 to 0.6 μM at P30, equivalent to an ~6-fold increase in sensitivity. In this study, we recorded odorant-induced inward currents in the dendritic knobs of individual OSNs, which represent a relatively direct measurement of the transduction events. It would be interesting to know how these transduction currents convert into action potentials which carry the odor information to the brain. We did not compare odorant-induced firing patterns in this study because we only observed action potentials in some but not all MOR23 neurons upon odorant stimulation under current-clamp mode. It is possible that some action potentials are generated relatively far out in the axon, and that they do not backpropagate into the soma and dendrites. The increased sensitivity of the primary sensory neurons potentially contributes to the improved smell ability at the behavioral level during postnatal development (Alberts and May, 1980b).

The most striking change of OSNs during the first postnatal month is that they exhibit increased selectivity (Fig. 5). MOR23 neurons from P9–P15 and P30 mice are relatively selective to lyral, consistent with previous ligand identification among a panel of diverse odorants (Touhara et al., 1999). Surprisingly, MOR23 neurons from P0 mice are broadly responsive to distinct odorants, often with amplitudes comparable or even larger than lyral responses. This phenomenon is unlikely restricted to the MOR23 receptor, because randomly recorded rodent OSNs become more selective during early development (Gesteland et al., 1982). At present, we can only speculate the underlying mechanisms. One possibility is that young OSNs start with multiple ORs and gradually one OR becomes dominant by suppressing the expression of other ORs. However, coexpression of multiple ORs or gene switching in OSNs is infrequently encountered even at early stages (Shykind et al., 2004; Tian and Ma, 2008). Another possibility is that OSNs from newborn mice use different signal transduction cascades compared with those from P30 mice. This is supported by the fact that newborn G_{olf}-null mice exhibit odorant-induced EOG signals, probably via signaling of other G-proteins (Belluscio et al., 1998; Lin et al., 2007). Other potential mechanisms underlying the selectivity difference between P0 and P30 include differential gap junction connections, mucus components (e.g., odorant binding proteins), and modification of odorant receptor proteins.

OMP has been widely used as a marker for mature OSNs since its initial identification (Margolis, 1972), but its functions are still elusive. Here we demonstrated that OSNs undergo a functional maturation process and OMP is required in this process. Deletion of OMP in OSNs from P30 animals leads to response properties resembling those from newborns in all three aspects tested. First,

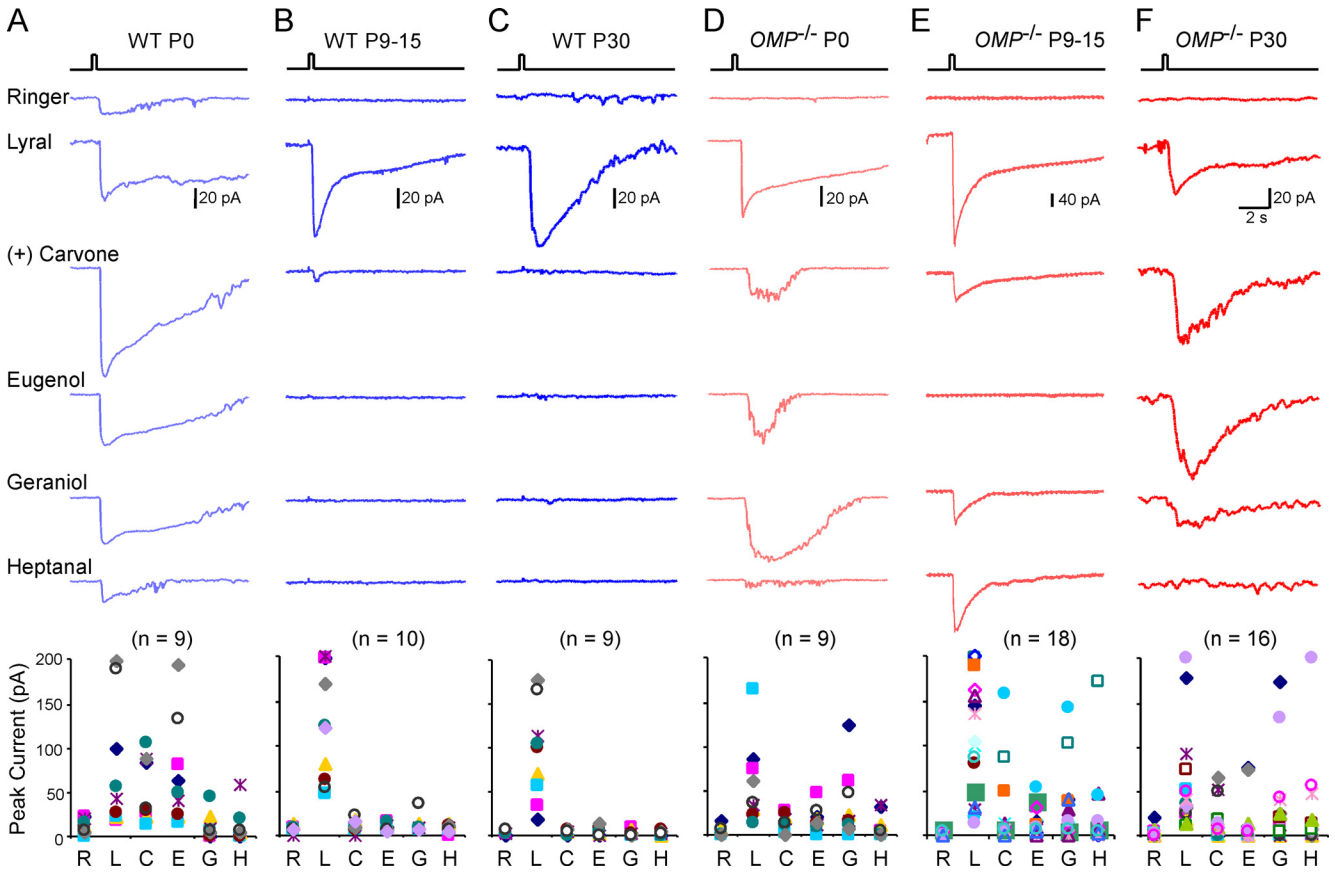

Figure 5. Wild-type but not $OMP^{-/-}$ MOR23 neurons increase the selectivity during the first month. ***A–F***, Odorant-induced transduction currents were recorded in MOR23 neurons under different conditions: WT P0 (***A***), WT P9 –P15 (***B***), WT P30 (***C***), $OMP^{-/-}$ P0 (***D***), $OMP^{-/-}$ P9 –P15 (***E***) and $OMP^{-/-}$ P30 (***F***). Each scatter plot in the bottom row shows the peak currents induced by different stimuli in individual cells under the corresponding condition. Each color represents a single cell. When a peak current exceeds 200 pA, it is plotted at 200 pA for the purpose of visualization. All odorants were delivered at 100 μM (except two cells in WT P0 tested by 10 μM) and the holding potential was −65 mV for all neurons.

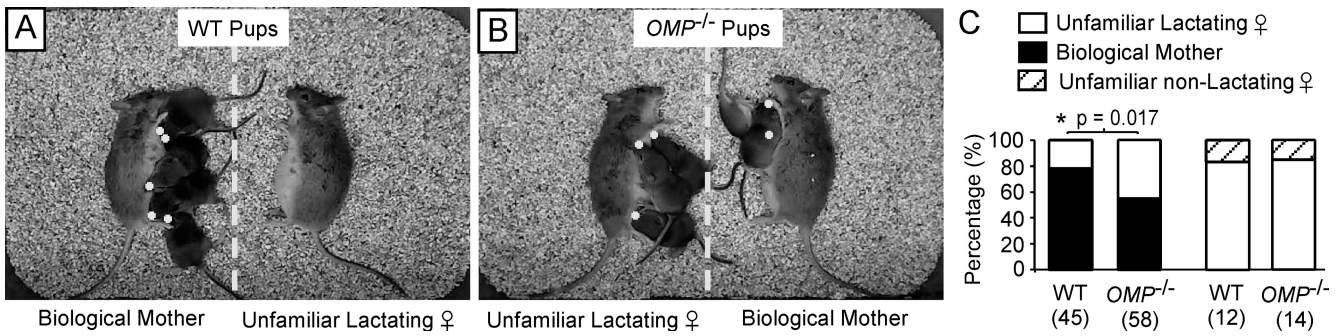

Figure 6. Wild-type but not $OMP^{-/-}$ pups prefer the biological mother. ***A***, ***B***, WT pups preferred to suckle or huddle with the biological mother over another unfamiliar lactating female (***A***), while $OMP^{-/-}$ mice failed to show preference (***B***). The nose of each pup is marked by a dot and its location relative to the midline (dashed line) between the two anesthetized mothers is used to assign the pup's preference. ***C***, Summary of mother preference for WT and $OMP^{-/-}$ pups. The numbers in parentheses indicate the total number of pups tested in each group. Statistical analysis was performed using a χ^2 test. The choice between a lactating and a nonlactating female (both are unfamiliar) was tested from two litters of each genotype.

the response kinetics (both activation and decay phase) is slower in $OMP^{-/-}$ neurons (Figs. 1, 2), which is consistent with previous EOG and single-cell recordings (Buiakova et al., 1996; Ivic et al., 2000; Reisert et al., 2007). This agreement suggests that the OMP-null phenotype in the current study should not be restricted to MOR23 neurons but generally applicable to OSNs expressing other ORs. Second, the response sensitivity is significantly reduced in $OMP^{-/-}$ OSNs. At P30, the sensitivity of MOR23 neurons in responding to lyral is ~7-fold higher with OMP ($K_{1/2} = 0.6$ μM) compared with that without OMP ($K_{1/2} = 4.2$ μM) (Fig. 4). The reduced sensitivity of $OMP^{-/-}$ OSNs may contribute to the higher detection threshold found in OMP-null mice in behavioral tests (Youngentob and Margolis, 1999), which can be rescued by viral transfection of OMP (Youngentob et al., 2004). Third, $OMP^{-/-}$ MOR23 neurons from P30 mice fail to become specific lyral detectors (Fig. 5). These data suggest that $OMP^{-/-}$ OSNs are functionally "locked" in an immature stage in odorant response properties. However, this does not imply that these properties are achieved by the same cellular mechanisms.

With the wide-range of deficits in $OMP^{-/-}$ OSNs, it is plausible that OMP exerts its molecular and cellular actions at multi-

ple sites. Our biochemical and pharmacological experiments support that ACIII is one of the proteins that is modulated by OMP deletion. Although the total ACIII level is upregulated in $OMP^{-/-}$ mice, odorant-induced phosphorylation of ACIII is reduced (Fig. 3), which potentially leads to slower termination of the responses (Wei et al., 1998). Indeed, blocking phosphorylation via a CaMKII inhibitor in WT OSNs mimics the slow termination in $OMP^{-/-}$ phenotype. Conversely, enhancing phosphorylation by blocking phosphatase activity restores the fast termination in $OMP^{-/-}$ OSNs (Fig. 3). Phosphatase 2A is likely involved in this process, because it is especially sensitive to okadaic acid (Kroner et al., 1996). Although the results of the pharmacological experiments are consistent with our hypothesis on modulation of ACIII in $OMP^{-/-}$ phenotype, there may be other proteins (such as odorant receptors) serving as substrates for phosphorylation and dephosphorylation (Boekhoff and Breer, 1992). Nevertheless, our results revealed a critical role of CaMKII and phosphatase 2A in determining the response kinetics in OSNs. OMP deletion also causes a trend of upregulation of PDE4A and β-arrestin-2 ($p = 0.07$ for both proteins in t test for Western blots expression levels), confirmed by immunostaining in the olfactory epithelium. PDE4A potentially helps to remove the intracellular cAMP (Cygnar and Zhao, 2009) and β-arrestin-2 is involved in OR desensitization (Mashukova et al., 2006). Further studies are needed to dissect out the contributions of each of these signaling proteins in OMP phenotype.

We used a simple mother preference test to investigate the potential impact of maturation of OSNs on early development of smell function in the animal. We found that WT pups (P7 to P16) preferred the biological mother to suckle or huddle with over an unfamiliar lactating female. In contrast, $OMP^{-/-}$ pups did not show preference, revealing a novel behavioral deficit in OMP knock-out mice (Fig. 6). This behavior is most likely mediated by olfactory cues because some of the pups did not open their eyes when the tests were performed. With both mothers anesthetized, it is unlikely the pups used auditory, thermal, or somatosensory cues to identify their biological mother.

Different odor-guided behaviors appear to function at different developmental stages and may be influenced by OMP deletion to different degrees. For instance, neonates rely on the olfactory cues to initiate suckling (Blass and Teicher, 1980) and $OMP^{-/-}$ pups are normal in this aspect. During the early postnatal period, rodent pups gradually develop preference for huddling with conspecifics (Alberts and Brunjes, 1978; Brunjes and Alberts, 1979), for home odors (Gregory and Pfaff, 1971), and for mother odors (Polan and Hofer, 1998). Here we demonstrated that WT mouse pups prefer their own mother over an unfamiliar lactating female (Fig. 6). A common feature of these behaviors is that rodent pups are attracted to familiar odors, which could result from genetic relatedness (Todrank et al., 2005) and/or experience-dependent learning (Wilson and Sullivan, 1994).

Genetic ablation of OMP leads to mouse pups that do not show preference for their biological mother, which likely results from disruption of the functional maturation process of OSNs. The results of the behavioral tests should extend beyond the special case of MOR23 mice. Curiously, the mere capability of OSNs in responding to odors is not sufficient for the pups to smell properly. For instance, odorant-induced EOG signals can be elicited from G_{olf} knock-out mice at P0, but these pups die from starvation shortly after birth. Our results on the selectivity of OSNs at P0 may have provided an explanation. When a large fraction of OSNs responds to many odorants in a nonselective manner, the animals have impaired capability to discriminate the odorants (Fleischmann et al., 2008). Similarly, $OMP^{-/-}$ OSNs can respond to odorants but with less selectivity (Fig. 5), which may be one of the factors leading to improper development of mother preference observed here.

References

Alberts JR, Brunjes PC (1978) Ontogeny of thermal and olfactory determinants of huddling in the rat. J Comp Physiol Psychol 92:897–906.

Alberts JR, May B (1980a) Development of nasal respiration and sniffing in the rat. Physiol Behav 24:957–963.

Alberts JR, May B (1980b) Ontogeny of olfaction: development of the rats' sensitivity to urine and amyl acetate. Physiol Behav 24:965–970.

Belluscio L, Gold GH, Nemes A, Axel R (1998) Mice deficient in G(olf) are anosmic. Neuron 20:69–81.

Blass EM, Teicher MH (1980) Suckling. Science 210:15–22.

Boekhoff I, Breer H (1992) Termination of second messenger signaling in olfaction. Proc Natl Acad Sci U S A 89:471–474.

Bozza T, McGann JP, Mombaerts P, Wachowiak M (2004) In vivo imaging of neuronal activity by targeted expression of a genetically encoded probe in the mouse. Neuron 42:9–21.

Brunet LJ, Gold GH, Ngai J (1996) General anosmia caused by a targeted disruption of the mouse olfactory cyclic nucleotide-gated cation channel. Neuron 17:681–693.

Brunjes PC, Alberts JR (1979) Olfactory stimulation induces filial preferences for huddling in rat pups. J Comp Physiol Psychol 93:548–555.

Buiakova OI, Baker H, Scott JW, Farbman A, Kream R, Grillo M, Franzen L, Richman M, Davis LM, Abbondanzo S, Stewart CL, Margolis FL (1996) Olfactory marker protein (OMP) gene deletion causes altered physiological activity of olfactory sensory neurons. Proc Natl Acad Sci U S A 93:9858–9863.

Cygnar KD, Zhao H (2009) Phosphodiesterase 1C is dispensable for rapid response termination of olfactory sensory neurons. Nat Neurosci 12:454–462.

Fleischmann A, Shykind BM, Sosulski DL, Franks KM, Glinka ME, Mei DF, Sun Y, Kirkland J, Mendelsohn M, Albers MW, Axel R (2008) Mice with a "monoclonal nose": perturbations in an olfactory map impair odor discrimination. Neuron 60:1068–1081.

Galef BG Jr, Henderson PW (1972) Mother's milk: a determinant of the feeding preferences of weaning rat pups. J Comp Physiol Psychol 78:213–219.

Gesteland RC, Yancey RA, Farbman AI (1982) Development of olfactory receptor neuron selectivity in the rat fetus. Neuroscience 7:3127–3136.

Graziadei GA, Stanley RS, Graziadei PP (1980) The olfactory marker protein in the olfactory system of the mouse during development. Neuroscience 5:1239–1252.

Gregory EH, Pfaff DW (1971) Development of olfactory-guided behavior in infant rats. Physiol Behav 6:573–576.

Grosmaitre X, Vassalli A, Mombaerts P, Shepherd GM, Ma M (2006) Odorant responses of olfactory sensory neurons expressing the odorant receptor MOR23: a patch clamp analysis in gene-targeted mice. Proc Natl Acad Sci U S A 103:1970–1975.

Grosmaitre X, Santarelli LC, Tan J, Luo M, Ma M (2007) Dual functions of mammalian olfactory sensory neurons as odor detectors and mechanical sensors. Nat Neurosci 10:348–354.

Ivic L, Pyrski MM, Margolis JW, Richards LJ, Firestein S, Margolis FL (2000) Adenoviral vector-mediated rescue of the OMP-null phenotype in vivo. Nat Neurosci 3:1113–1120.

Kroner C, Boekhoff I, Breer H (1996) Phosphatase 2A regulates the responsiveness of olfactory cilia. Biochim Biophys Acta 1312:169–175.

Kwon HJ, Koo JH, Zufall F, Leinders-Zufall T, Margolis FL (2009) Ca extrusion by NCX is compromised in olfactory sensory neurons of OMP mice. PLoS One 4:e4260.

Lin W, Margolskee R, Donnert G, Hell SW, Restrepo D (2007) Olfactory neurons expressing transient receptor potential channel M5 (TRPM5) are involved in sensing semiochemicals. Proc Natl Acad Sci U S A 104:2471–2476.

Ma M, Chen WR, Shepherd GM (1999) Electrophysiological characterization of rat and mouse olfactory receptor neurons from an intact epithelial preparation. J Neurosci Methods 92:31–40.

Margolis FL (1972) A brain protein unique to the olfactory bulb. Proc Natl Acad Sci U S A 69:1221–1224.

Mashukova A, Spehr M, Hatt H, Neuhaus EM (2006) Beta-arrestin2-

mediated internalization of mammalian odorant receptors. J Neurosci 26:9902–9912.

Moriceau S, Sullivan RM (2006) Maternal presence serves as a switch between learning fear and attraction in infancy. Nat Neurosci 9:1004–1006.

Pace U, Hanski E, Salomon Y, Lancet D (1985) Odorant-sensitive adenylate cyclase may mediate olfactory reception. Nature 316:255–258.

Polan HJ, Hofer MA (1998) Olfactory preference for mother over home nest shavings by newborn rats. Dev Psychobiol 33:5–20.

Reisert J, Yau KW, Margolis FL (2007) Olfactory marker protein modulates the cAMP kinetics of the odour-induced response in cilia of mouse olfactory receptor neurons. J Physiol 585:731–740.

Schapiro S, Salas M (1970) Behavioral response of infant rats to maternal odor. Physiol Behav 5:815–817.

Shykind BM, Rohani SC, O'Donnell S, Nemes A, Mendelsohn M, Sun Y, Axel R, Barnea G (2004) Gene switching and the stability of odorant receptor gene choice. Cell 117:801–815.

Sklar PB, Anholt RR, Snyder SH (1986) The odorant-sensitive adenylate cyclase of olfactory receptor cells. Differential stimulation by distinct classes of odorants. J Biol Chem 261:15538–15543.

Su CY, Menuz K, Carlson JR (2009) Olfactory perception: receptors, cells, and circuits. Cell 139:45–59.

Tian H, Ma M (2008) Activity plays a role in eliminating olfactory sensory neurons expressing multiple odorant receptors in the mouse septal organ. Mol Cell Neurosci 38:484–488.

Todrank J, Busquet N, Baudoin C, Heth G (2005) Preferences of newborn mice for odours indicating closer genetic relatedness: is experience necessary? Proc Biol Sci 272:2083–2088.

Touhara K, Vosshall LB (2009) Sensing odorants and pheromones with chemosensory receptors. Annu Rev Physiol 71:307–332.

Touhara K, Sengoku S, Inaki K, Tsuboi A, Hirono J, Sato T, Sakano H, Haga T (1999) Functional identification and reconstitution of an odorant receptor in single olfactory neurons. Proc Natl Acad Sci U S A 96:4040–4045.

Vassalli A, Rothman A, Feinstein P, Zapotocky M, Mombaerts P (2002) Minigenes impart odorant receptor-specific axon guidance in the olfactory bulb. Neuron 35:681–696.

Wei J, Zhao AZ, Chan GC, Baker LP, Impey S, Beavo JA, Storm DR (1998) Phosphorylation and inhibition of olfactory adenylyl cyclase by CaM kinase II in Neurons: a mechanism for attenuation of olfactory signals. Neuron 21:495–504.

Welker WI (1964) Analysis of sniffing of the albino rat. Behaviour 22:223–244.

Wilson DA, Sullivan RM (1994) Neurobiology of associative learning in the neonate: early olfactory learning. Behav Neural Biol 61:1–18.

Wong ST, Trinh K, Hacker B, Chan GC, Lowe G, Gaggar A, Xia Z, Gold GH, Storm DR (2000) Disruption of the type III adenylyl cyclase gene leads to peripheral and behavioral anosmia in transgenic mice. Neuron 27:487–497.

Youngentob SL, Margolis FL (1999) OMP gene deletion causes an elevation in behavioral threshold sensitivity. Neuroreport 10:15–19.

Youngentob SL, Margolis FL, Youngentob LM (2001) OMP gene deletion results in an alteration in odorant quality perception. Behav Neurosci 115:626–631.

Youngentob SL, Pyrski MM, Margolis FL (2004) Adenoviral vector-mediated rescue of the OMP-null behavioral phenotype: enhancement of odorant threshold sensitivity. Behav Neurosci 118:636–642.